

Mineral dust – natural and anthropogenic

- Anthropogenic dust sources:**
Dust sources associated with agricultural land use
 - Considered: Mineral dust only (no urban pollution)
 - Not considered: Emissions from vehicles (dirt roads, tillage, recreational use); military operations
 - Not considered: Indirect anthropogenic sources, e.g. hydrological
- Dust emissions from anthropogenic sources can impact daily life, not only in (semi-)arid areas
 - 1930s Dust Bowl, USA (**Fig. 1a**)
 - Traffic accidents, e.g. 2011 in northern Germany (**Fig. 1b**)



Fig. 1: (a) "Dust Bowl" in the US (image credit: Arthur Rothstein/Wikipedia); (b) Pile-up on a highway in Germany caused by a dust storm in 2011 (image credit: spiegel.de)

Global impacts?

- The contribution of (anthropogenic) land use to present-day dust emission remains under debate, with values ranging from 10% to 50% (e.g. Tegen and Fung, 1995; Sokolik and Toon, 1996; Tegen et al., 2004; Mahowald et al., 2004)
- Ginoux et al. (2012) estimated that anthropogenic sources contribute 25% to total dust emissions
 - Areas with > 30% land use (HYDE 2, Klein Goldewijk, 2001) were considered as anthropogenic sources
 - FoO of MODIS DeepBlue dust optical depth (DOD) exceeding a threshold of 0.2
 - Resolution $0.1^\circ \times 0.1^\circ$
 - Offline dust emissions: Ginoux et al. (2001): parameterization with uniform threshold wind speeds, combined with FoO

Objectives and Methods

We aim to better estimate the contributions of anthropogenic (agricultural) and natural sources to global dust emission by combining improved land-surface representations with advanced dust models and observational constraints

- Updated land-use data set (HYDE 3.2.1, Klein Goldewijk et al., 2017)
- Fully coupled dust emission parameterizations
- Dynamic threshold friction velocity for sediment entrainment
- Satellite-based representation of photosynthetic and non-photosynthetic vegetation cover
- 4D dust concentration field allowing in-depth evaluation

Numerical Experiments

Model and Setup

- Multiscale Online Non-hydrostatic Atmosphere RE Chemistry model – NMMB-MONARCH (Pérez et al., 2011; Badia et al., 2017)
- Global setup ($1^\circ \times 1.4^\circ$ horizontal resolution, 24 layers)
- Initially one-year simulations (2012)
- We use four different dust emission parameterizations (cf. **Fig. 2**) to quantify uncertainty arising from the emission scheme.

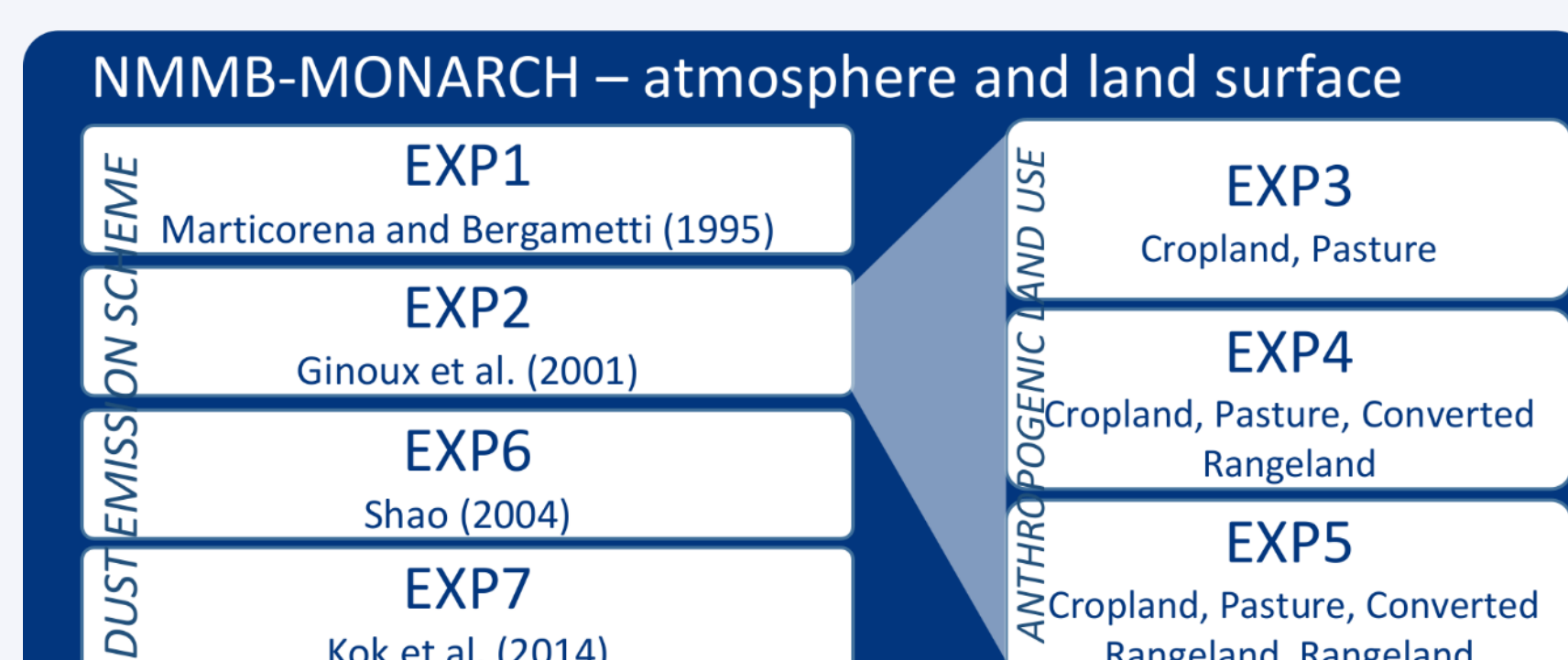


Fig. 2: Overview of the numerical experiments designed to constrain the contribution of anthropogenic sources to the global dust cycle.

Drag Partitioning

- "Drag partition" = separation of the total (surface) drag supplied by aerodynamic forces into a fraction on roughness element surfaces and on the ground surface. The latter is pivotal for dust emission.
- Drag partition is used to account for the effect of roughness elements, such as vegetation, on the emission.
- We use the drag partition parameterization of Raupach et al. (1993) in combination with estimates of photosynthetic (PV) and non-photosynthetic (NPV) vegetation cover (Guerschman et al., 2015) and the conversion between cover fraction and frontal area index (input to the drag partition scheme) proposed by Shao et al. (1996).
- The roughness correction factor and the frequency of occurrence (FoO) of dust optical depth > 0.2 (Ginoux et al., 2012) are remarkably similar (**Fig. 3**), demonstrating that roughness element cover and a dynamical representation of u_{*t} is key to reproduce observed atmospheric dust loadings.

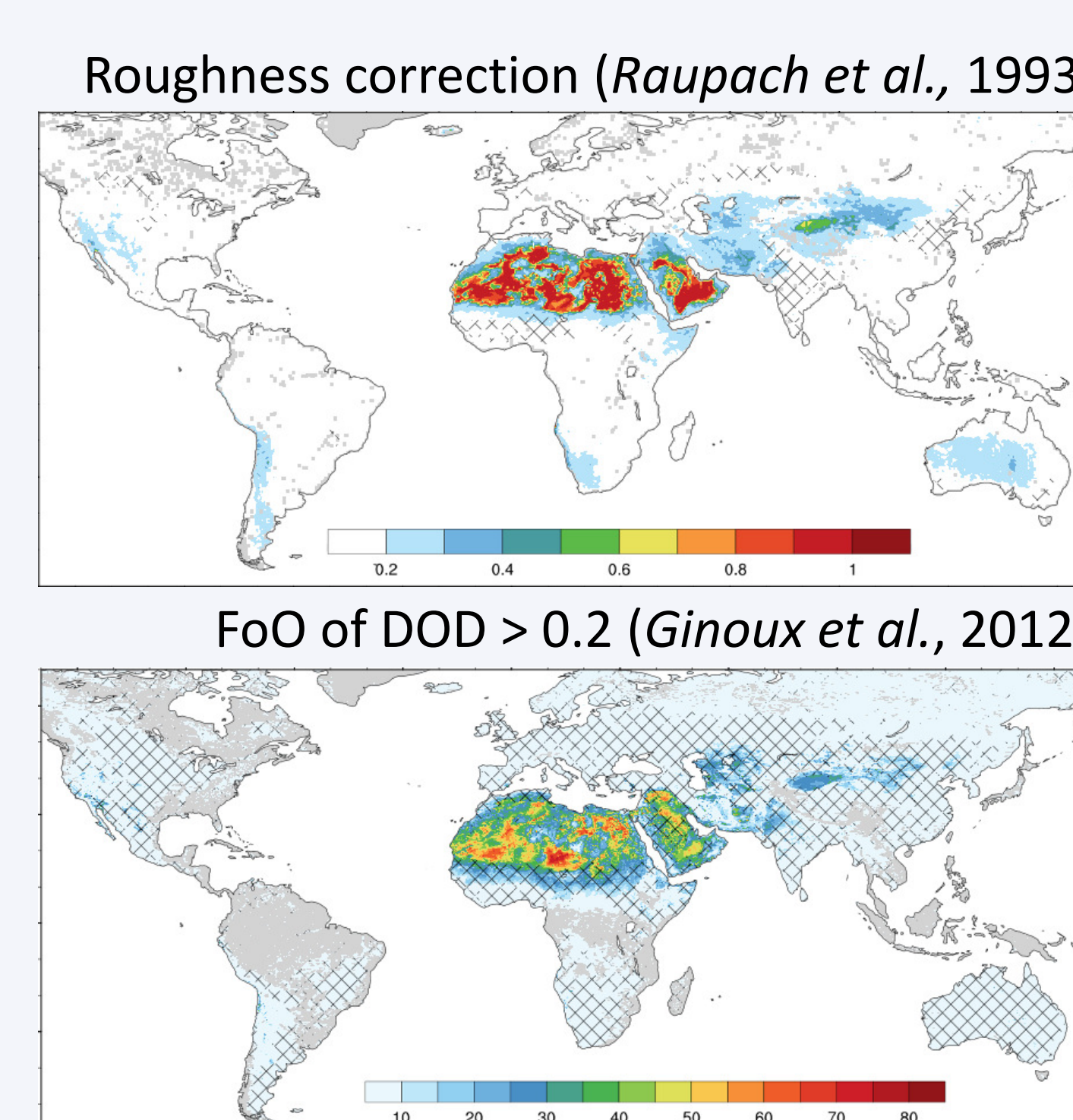


Fig. 3: (top) Correction factor representing roughness elements; the factor is applied to the entrainment threshold friction velocity; (bottom) Frequency of occurrence (FoO) of dust optical depth (DOD) > 0.2 .

Anthropogenic land use

- HYDE 3.2.1 (Klein Goldewijk et al., 2017)**
- Data on annual basis; spatial resolution $\sim 0.1^\circ$ resolution
- Land use categories considered here:
 - Cropland:** Arable land and permanent crops
 - Pasture:** grazing land with an aridity index > 0.5 , intensively used/managed
 - Converted Rangeland:** grazing land placed on potential forest area, less intensively used
 - Rangeland:** natural, unconverted grazing land with an aridity index < 0.5 , less or unmanaged
- Land-use configurations tested (**Fig. 4**):
 - (LU1)** Cropland, pasture
 - (LU2)** Cropland, pasture, converted rangeland
 - (LU3)** Cropland, pasture, converted rangeland, rangeland

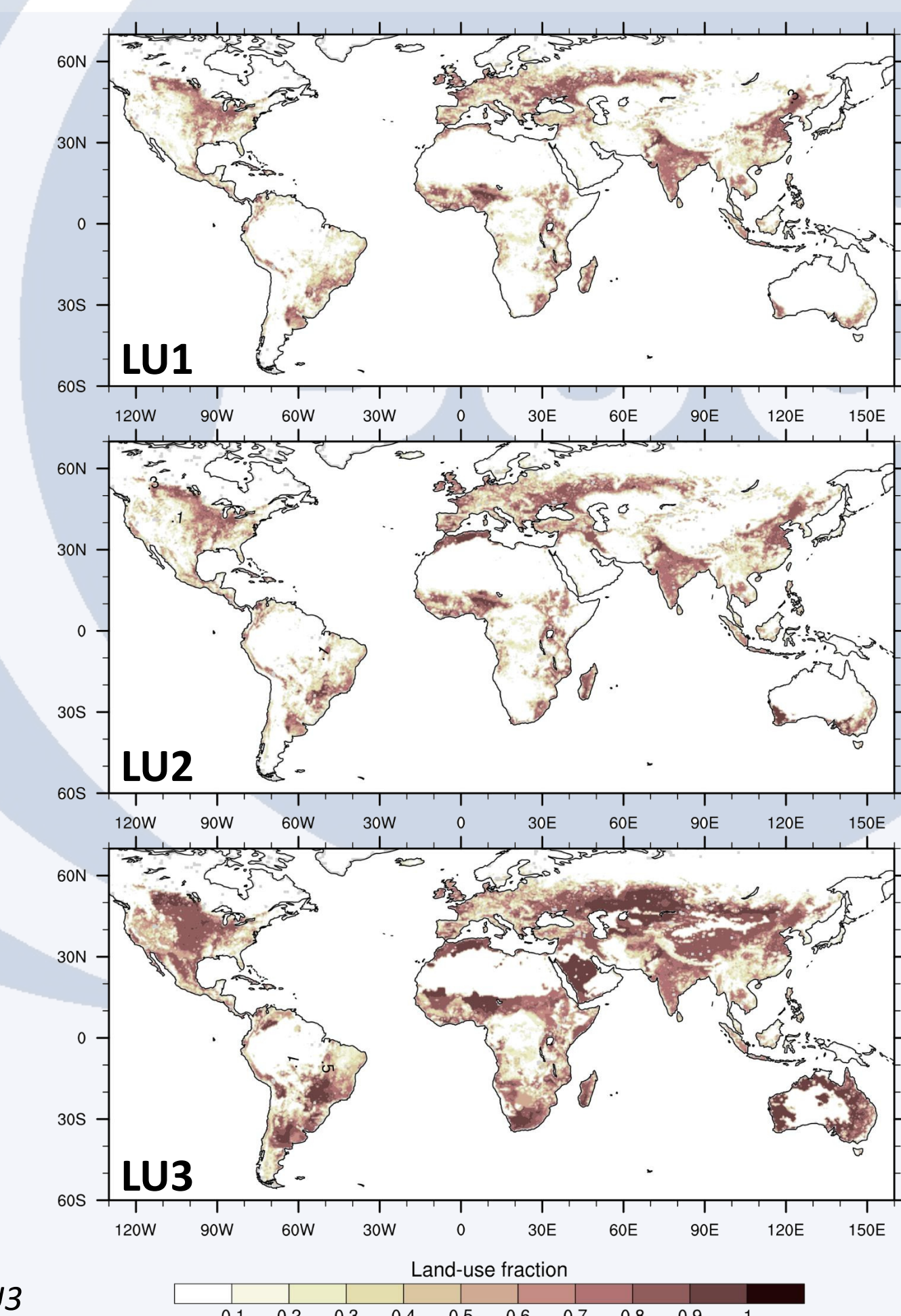


Fig. 4: Land-use fractions obtained using configurations LU1 – LU3

Results

Dust optical depth – MODIS and MONARCH

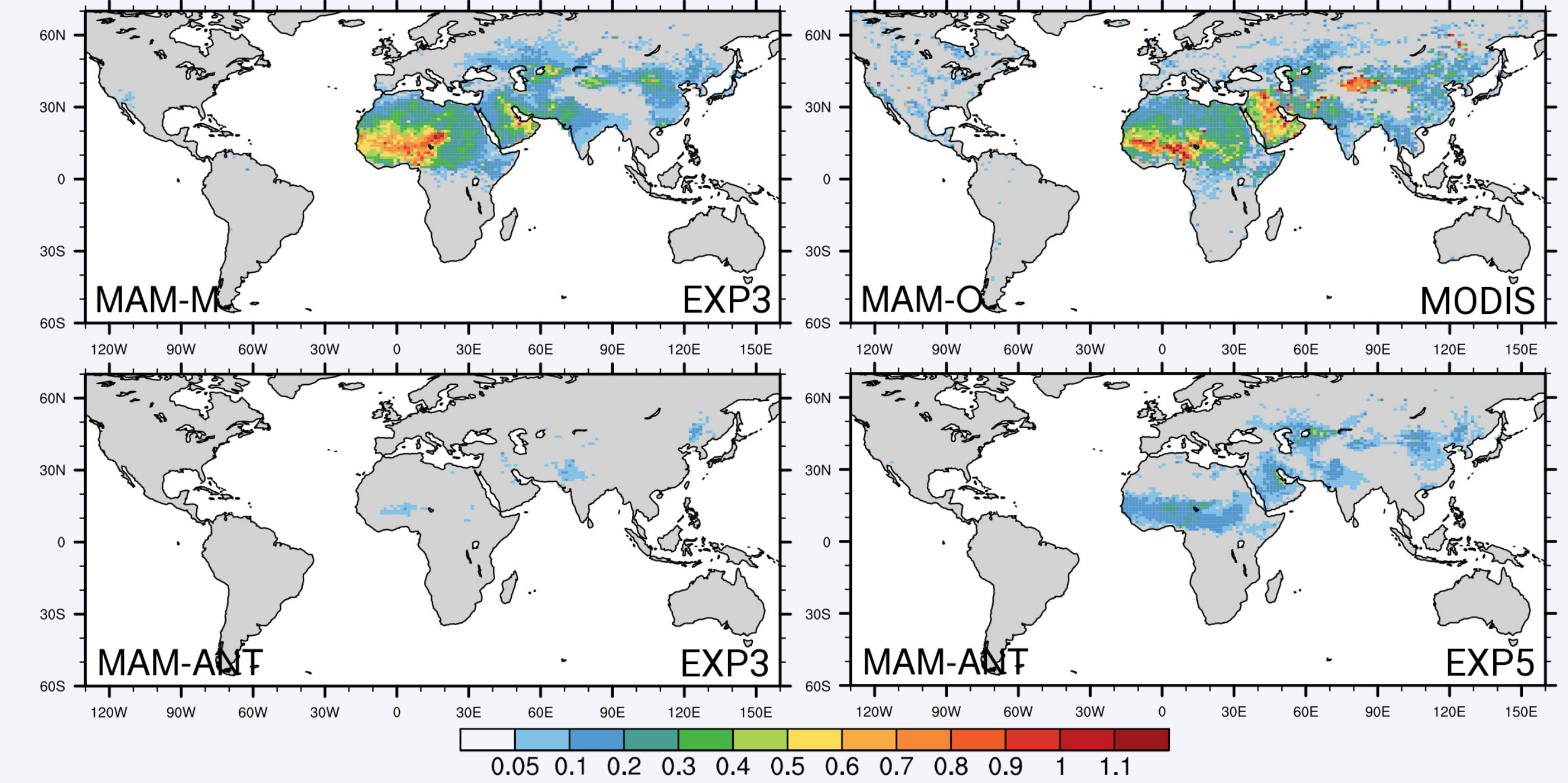


Fig. 5: Total dust optical depth for northern hemispheric spring (March, April, May) obtained using EXP3 (top-left) together with the corresponding anthropogenic fractions based on EXP3 (bottom-left) and EXP5 (bottom-right). MODIS Deep Blue dust optical depth is shown as a reference (top-right).

- Spatio-temporal co-location between MODIS and model data
- Good agreement between model and observations
- Slight underestimation of DOD in the Arabian Peninsula and the Taklamakan Desert; slight overestimation around the Bodele Depression
- The contribution of anthropogenic sources is minor when considering cropland and pasture only (LU1); the addition of rangeland (LU3) yields a substantial increase in anthropogenic dust.
- Extent of anthropogenic source area determines seasonal variability of anthropogenic dust contribution (not shown).

Dust emission – anthropogenic contribution

- Global anthropogenic fraction on average 8% when using emission scheme from Ginoux et al. (2001) and HYDE 3.2.1 cropland and pasture (EXP3).
- Considering rangeland as anthropogenic source leads to estimate of about 35%, similar to that using HYDE 2 (cropland and pasture) → large uncertainty due to definition of "anthropogenic sources".
- The largest anthropogenic emission fractions are found in North America, Southwest Asia, and Europe, although the contributions of these areas to the dust cycle are small (**Tab. 1**).
- The large uncertainty associated with the anthropogenic emission fractions listed in **Tab. 1** is due to the different land-use configurations.
- Inclusion of additional dust emission parameterizations will lead to larger variability of both the regional contribution to total emission and the anthropogenic emission fraction and will help to better constrain the uncertainty.

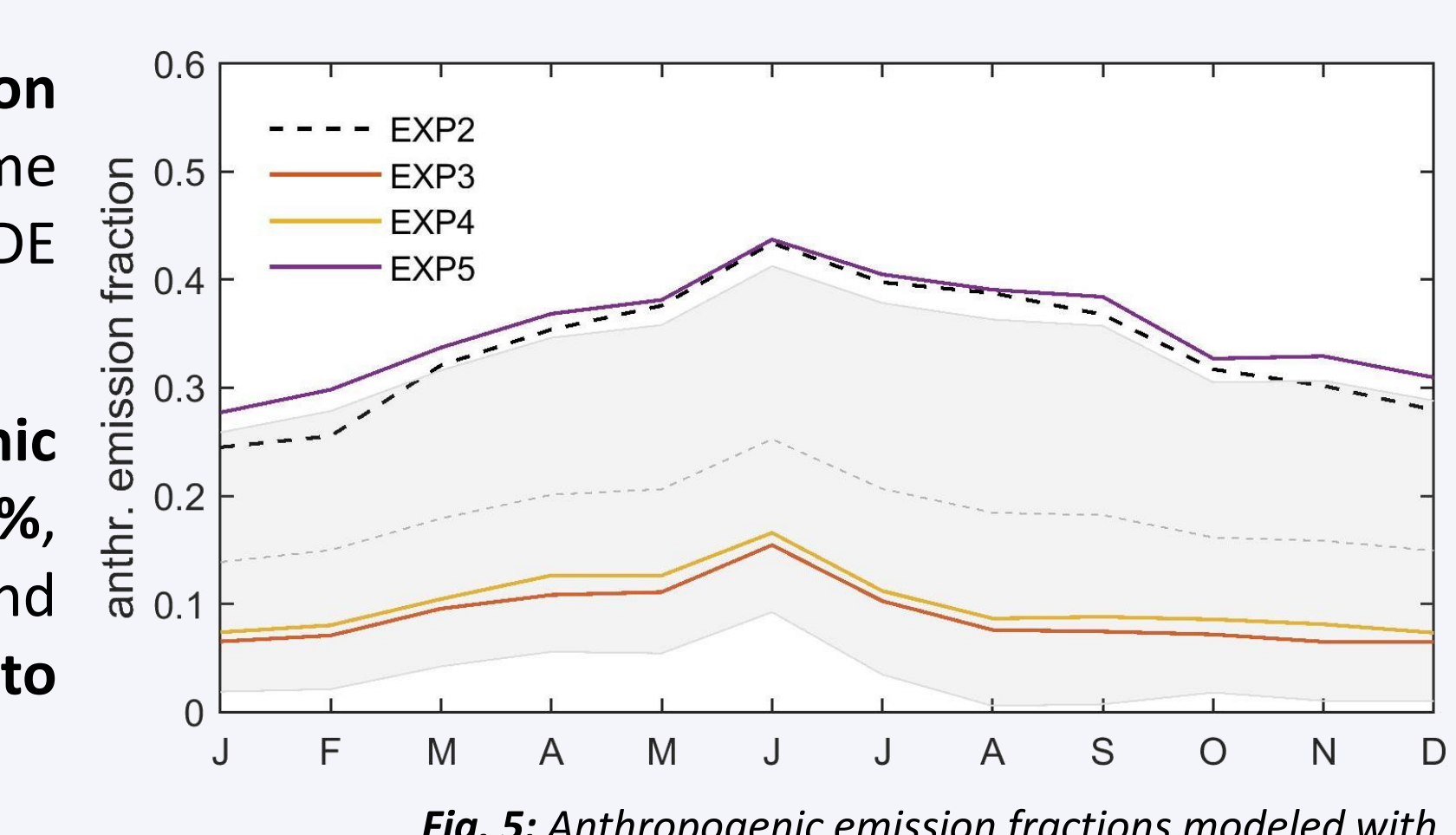


Fig. 5: Anthropogenic emission fractions modeled with NMMB-MONARCH based on EXPs 2-5.

Region	Anthro. emission fraction (avg ± std)	Regional contribution to total emission (avg ± std)
N Africa	10.8 ± 9.3	50.6 ± 0.2
S Africa	0.2 ± 0.3	0.2 ± 0.0
Middle East	21.1 ± 21.7	28.2 ± 0.1
NW Asia	27.6 ± 32.9	8.6 ± 0.0
SW Asia	47.0 ± 3.2	5.3 ± 0.0
NE Asia	33.8 ± 20.2	8.9 ± 0.0
Australia	17.1 ± 19.6	0.2 ± 0.1
S America	27.9 ± 22.9	1.2 ± 0.3
N America	47.1 ± 19.9	1.5 ± 0.1
Europe	43.4 ± 17.0	2.4 ± 0.0

Tab. 1: Regional fractions of anthropogenic emissions together with the regional contributions to global dust emissions. Averages and standard deviations are based on EXPs 3-5.

Conclusions and Outlook

- Anthropogenic dust sources contribute to the global dust load.
- The main uncertainties are due to the land-surface condition, dust emission, and meteorological dust drivers.
- Diverse numerical experiments and thorough comparison with observations help to constrain the anthropogenic emission fraction.